

Direct wintertime pCO₂ observations from the Saildrone Gulf Stream Mission

Sarah Nickford & Jaime Palter, University of Rhode Island – Graduate School of Oceanography
Ocean Carbon and Biogeochemistry 2019 Meeting- supplemental information



Table of Contents:

- I. Abstract
- II. Mission details
- III. Calibration exercises
- IV. Stream coordinates & the first Saildrone Gulf Stream Crossing
- V. A comparison of observations to climatological estimates of $\Delta p\text{CO}_2$
- VI. Figures
- VII. Acknowledgements
- VIII. References

I. Abstract

Western boundary currents, such as the Gulf Stream, are thought to be hot spots of ocean carbon dioxide uptake. In these regions, the maximum CO₂ flux occurs wintertime, when in-situ observations are most sparse due to intense weather conditions that challenge sampling from ships. Moreover, the short spatial and temporal scales of variability require dense sampling to resolve the influence of the currents on gas exchange. We show the capability of an Autonomous Surface Vehicle (ASV), called Saildrone, for collecting transformative measurements in the Gulf Stream region during a February 2019 deployment. The Saildrone is a high-endurance (>3 months), fast moving (1-8 knots) ASV that carries a large payload of meteorological and oceanographic sensors. For our deployment, it was equipped with the PMEL-designed ASVCO₂ system, which measures pCO₂ in both the atmosphere and the ocean with climate-quality (2 µatm) accuracy using 2-point calibrations before every measurement. With pCO₂, sea surface temperature, salinity, and near-surface wind measurements, we calculate CO₂ fluxes in the cold, nutrient rich Slope Sea, across the Gulf Stream, and into the warm, nutrient poor Sargasso Sea during active convection. On our planned 30-day mission, Saildrone collected 18 days of pCO₂ data as it completed five crossings of the Gulf Stream before 7 m waves caused a leak in the ASVCO₂ system. We find that atmospheric pCO₂ varies by 22 µatm while oceanic pCO₂ varies by 43 µatm. The measured air-sea gradient in pCO₂ ($\Delta p\text{CO}_2$) averages -51.3 µatm, which is 38% higher than the February climatology of Takahashi (2009) and 59% higher than that of Landschutzer et al. (2013) in the same region, implying a greater ocean uptake than would be inferred from the climatologies. We hypothesize that the $\Delta p\text{CO}_2$ in such climatologies may be biased because of chronic under-sampling in winter when heat loss drives a strong increase in oceanic CO₂ solubility and vertical nutrient fluxes stimulate enhanced phytoplankton productivity.

II. Mission details

Saildrone

The Saildrone was launched from Newport Shipyard at 1pm on January 30th, 2019. Soon after launching, Saildrone encountered its first storm while on the shelf of the US East Coast, causing sensors to freeze. It completed a total of five crossings of the Gulf Stream (Figure 1). Later on in the mission, a storm built up starting on 2019-02-18 and subjected the Saildrone to 7 m seas and wind gusts up to 58 kts, ultimately leading to the failure of the ASVCO₂ sensor at 13:17:00 UTC on 2019-02-20. Following this event, the Durafet (pH sensor) continued to sample until 15:17:00 UTC on 2019-02-21, extending our data collection by an additional 24 hours. Due to these events, calibration exercises during the R/V Endeavor Cruise were not possible which lead us to the calibration exercises described in Section III.

R/V Endeavor

Despite the loss of functioning sensors on the Saildrone, we utilized our time on the R/V Endeavor to sample gradients near the Gulf Stream. The Endeavor left St. Georges, Bermuda on February 27th, 2019 and returned on March 4th, 2019. During the time of the cruise, the Saildrone was under an intense storm, bringing wind speeds of 58 kts and a significant wave height of 12.6 m. Due to the weather conditions and sea state, we were unable to meet up with the Saildrone,

so we went northwest of Bermuda (Figure 1). We had an underway CTD (thanks to Dave Ullman, URI), SAMI pCO₂ sensor (curtesy of Nick Bates and Becky Garley, BIOS), and SUMO pH/Nitrate sensor (Yui Takeshita, Jacki Long, Andrea Fassbender, MBARI). At this time, we have not calibrated the SAMI pCO₂ data. The pCO₂ data presented in this work was calculated using the SUMO pH data and estimated Total Alkalinity. This estimate compares well with discrete DIC samples taken during the cruise.

III. Calibration exercises

Our post-mission “calibration” consisted of calculating pH with CO2SYS using pCO₂ measured from the ASVCO2 and alkalinity estimated using the salinity relationship (Fassbender et al., 2017). We selected two time periods when the sensor was consistently working well. The first was 00:17:00 UTC on 2019-02-07 to 23:17:00 UTC on 2019-02-07, and the second, 00:17:00 UTC on 2019-02-17 to 23:17:00 UTC on 2019-02-17. During the two selected periods, the data collected by the ASVCO2 is assumed to be our “calibration samples.” This allows us to compare this section of data with the pH_{ext} corrected according to Martz et al., (2010) (corrections were performed by Stacy Maenner), to get an average offset value. The offset calculated from the first “calibration sample” [0.1645] was then added to the pH_{ext} corrected according to Martz (2010) for the time period after the sensor thawed (2019-02-02 14:17:00 UTC) until 2019-02-16 04:17:00 UTC when we noticed unrealistic pH variations recorded by the DuraFet. The second “calibration sample” offset [0.1380] was applied to the remainder of the data (Figure 2). It is possible that the sensor experienced drift which would explain the differences between measured and calibrated data starting on 2/11/2019 as well as the need for two “calibration samples.” Large excursions from the estimated pH are eliminated by removing values that differ by 0.015 or greater. We simultaneously remove the pCO₂ measurements at these points.

With the “calibrated” pH and calculated TA, we calculate seawater pCO₂ using CO2SYS (Figure 3). There are some differences between the measured and calculated seawater pCO₂ but this could be a result of standard uncertainty associated with the measurement (Williams et al., 2017).

IV. Stream coordinates & the first Saildrone Gulf Stream Crossing

In order to put meaningful physical context to the Saildrone data, we display it in the form of Gulf Stream crossings. These are created by taking the zonal velocity field and finding where the current reverses direction (begins to go westward) on either side of one crossing. These locations become start and endpoints for a crossing. Then, the depth-averaged velocity maximum is used to find the Gulf Stream core, in which velocities will be rotated along in order to get the data into the widely used stream coordinate system (Halkin et al., 1985). Next, we get the cross-stream distance axis by projecting the distance axis (as a function of cumulative distance from the Gulf Stream) onto the cross-stream axis. The sign convention is as follows: negative distances are to the south of the Gulf Stream (Sargasso Sea) and positive distances are to the north of the Gulf Stream (Slope Sea), therefore each crossing is viewed in the same orientation.

The first Saildrone Gulf Stream Crossing

The SSTs show a clear indication of the thermal north wall at 40 km north of the Gulf Stream core. The north wall is also prevalent as a sharp gradient in O₂ and salinity at the same location.

It appears as though there is more variability in O_2 north of the Gulf Stream when compared to that on the south side. It is challenging to note any distinguishable features in the pCO_2 in the three different regimes however, 10-minute pH data may provide higher spatial resolution which could make features appear more distinguishable. The CO_2 flux during this crossing was always negative (into the ocean) and is extremely dependent on the wind speed (Figure 4).

V. A comparison of observations to climatological estimates of ΔpCO_2

We focus on the comparison of ΔpCO_2 observations to climatological values rather than that of the CO_2 flux because of its extreme dependency on the wind speed. The Flux of CO_2 is represented by the equation:

$$F_{CO_2} = k * \alpha * \Delta pCO_2,$$

where k is the CO_2 transfer velocity ($k = 0.31 * U^{10^2} * \left(\frac{Sc}{660}\right)^{-0.5}$), α is the CO_2 solubility in seawater (function of temperature and salinity), and $\Delta pCO_2 = pCO_2^{ocean} - pCO_2^{atm}$. In order to make an accurate comparison of CO_2 fluxes, we would need to use the same climatological winds with our observed temperature, salinity, and ΔpCO_2 .

Climatological estimates show ΔpCO_2 in the Gulf Stream region of $-37 \mu atm$ based on Takahashi et al., (2009) and $-32 \mu atm$ based on Landschützer et al., (2013). The average ΔpCO_2 measured during the Saildrone Gulf Stream Mission is $-51 \mu atm$, implying a greater ocean uptake than inferred from the climatological estimates by 38% and 59%, respectively. In the subtropical interior, climatological estimates show the ΔpCO_2 at $-38 \mu atm$ and $-37 \mu atm$, respectively. The observations from the R/V Endeavor cruise indicate an average ΔpCO_2 of $-48 \mu atm$ suggesting they are 26% and 30% greater, respectively. The subtropical interior appears to be better represented in the climatological estimates, potentially as a result of a larger number of measurements due to routine BATS cruises. These observations may lead to an upward revision of western boundary current CO_2 uptake.

VI. Figures

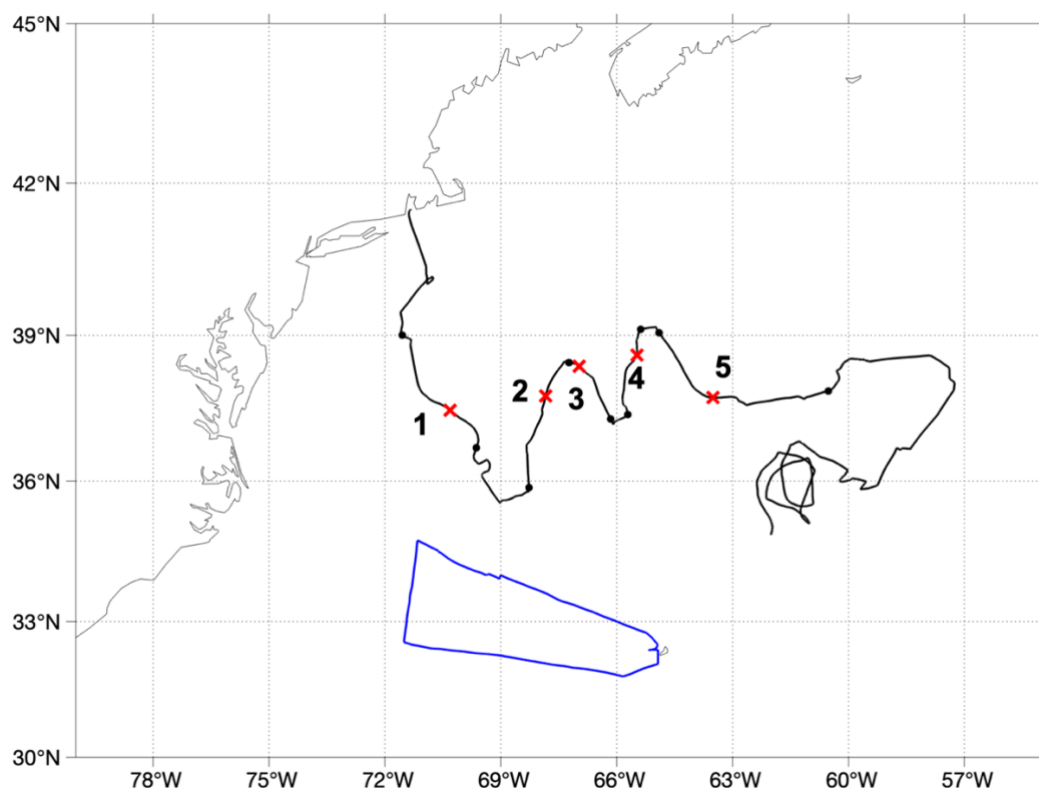


Figure 1. Saildrone Mission track (black) and Endeavor cruise track (blue). Locations of each crossing of the Gulf Stream by Saildrone during the 2019 mission, labeled in order of occurrence. Black dots indicate start/end points of a crossing, red X's indicate the location of the depth integrated velocity maximum for each crossing (location of the center of the Gulf Stream).

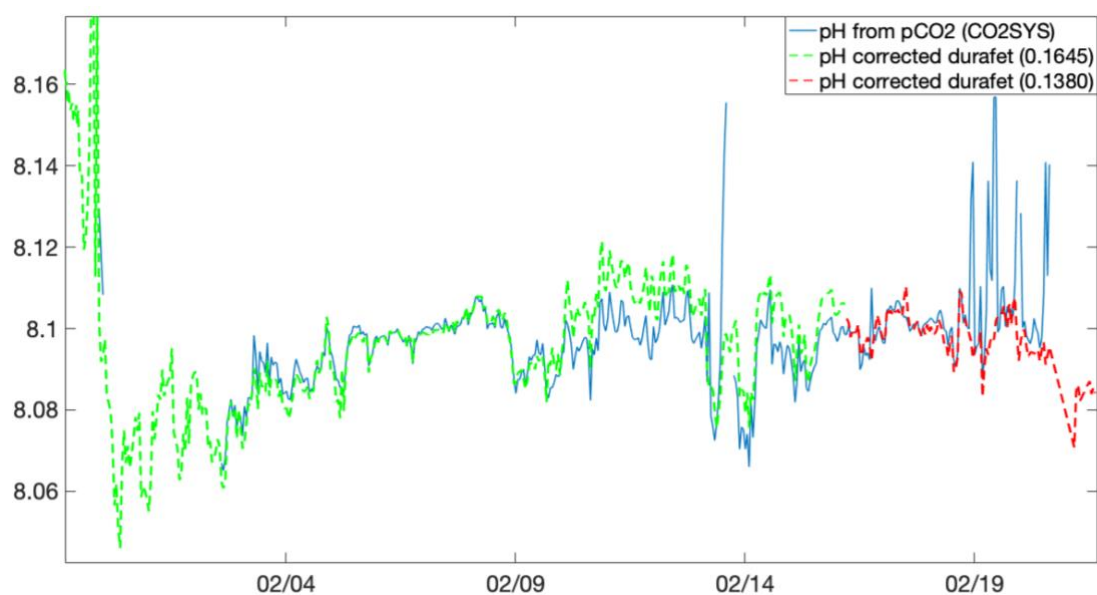


Figure 2. Corrected pH data using Martz (2010) and post-mission calibration measures as described in Section III.

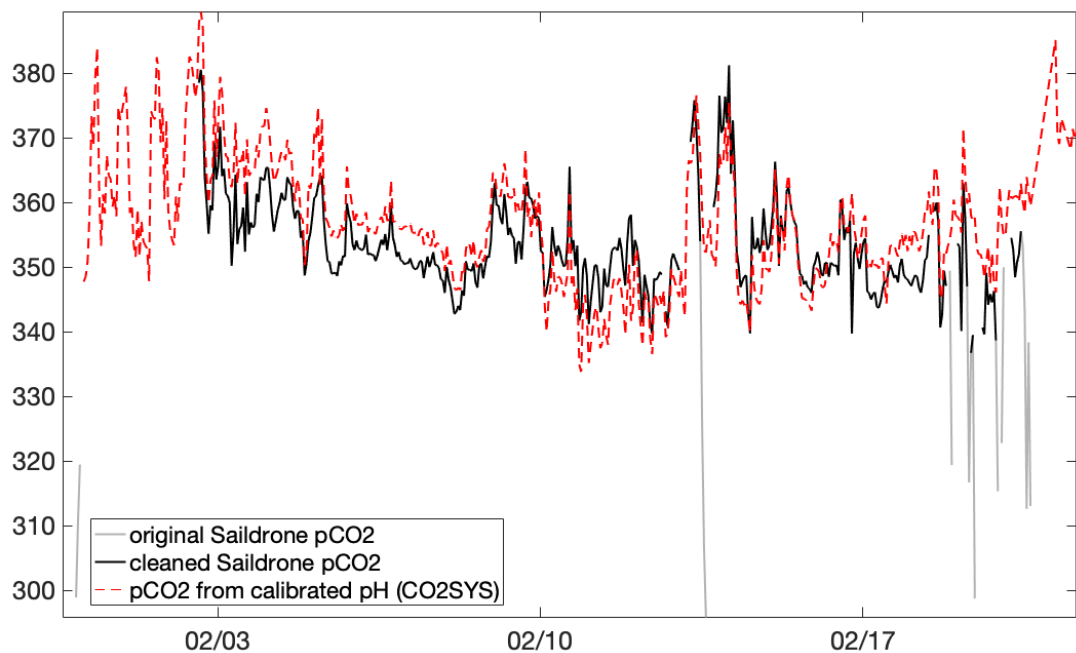


Figure 3. Timeseries of original $p\text{CO}_2$, cleaned $p\text{CO}_2$, and $p\text{CO}_2$ calculated from “calibrated” pH and estimated Total Alkalinity.

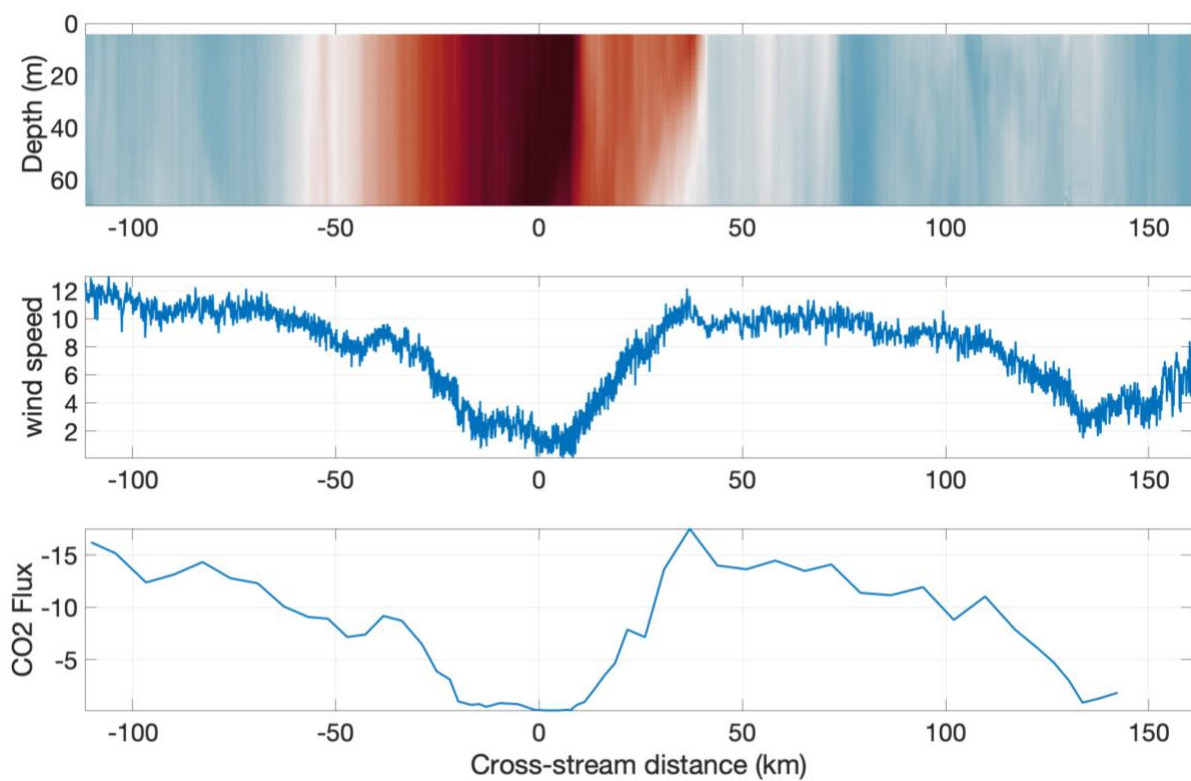


Figure 4. Along-stream velocity, wind speed and CO_2 flux for the first Gulf Stream crossing. The CO_2 flux is plotted using a reversed y-axis. All variables are plotted versus cross-Gulf Stream

distance, where the origin is at the position of the maximum depth-averaged velocity and distances are calculated normal to the velocity vector at that maximum.

VII. Acknowledgements

The 2018 Saildrone Award and the NSF RAPID Award made this research possible, along with important contributions from Kathy Donohue, Andrea Fassbender, Alison Gray, Jacki Long, Stacy Maenner, and Adrienne Sutton who participated in scientific planning, data collection, processing, and analysis advice. Thanks also to Nick Bates, Becky Garley, Yui Takeshita, and Dave Ullman for their help with instrumenting the R/V Endeavor cruise.

VIII. References

- Crameri, F. (2018a), Scientific colour-maps. Zenodo. <http://doi.org/10.5281/zenodo.1243862>
- Crameri, F. (2018b), Geodynamic diagnostics, scientific visualisation and StagLab 3.0, Geosci. *Model Dev.*, 11, 2541–2562, doi:10.5194/gmd-11-2541-2018
- Fassbender, A. J., Alin, S. R., Feely, R. A., Sutton, A. J., Newton, J. A., & Byrne, R. H. (2017). Estimating Total Alkalinity in the Washington State Coastal Zone: Complexities and Surprising Utility for Ocean Acidification Research. *Estuaries and Coasts*, 40(2), 404–418. <https://doi.org/10.1007/s12237-016-0168-z>
- Halkin, D., Rossby, H. T., & Rossby, T. (1985). Structure and Transport of the Gulf Stream at 73 N. *JPhysOceanogr*. [https://doi.org/10.1175/1520-0485\(1985\)015<1439:TSATOT>2.0.CO;2](https://doi.org/10.1175/1520-0485(1985)015<1439:TSATOT>2.0.CO;2)
- Landschützer, P., Gruber, N., Payne, M. R., Schuster, U., Bakker, D. C. E., Nakaoka, S., et al. (2013). A neural network-based estimate of the seasonal to inter-annual variability of the Atlantic Ocean carbon sink. *Biogeosciences*, 10(11), 7793–7815. <https://doi.org/10.5194/bg-10-7793-2013>
- Martz, T. R., Connery, J. G., & Johnson, K. S. (2010). Testing the Honeywell Durafet® for seawater pH applications. *Limnology and Oceanography: Methods*, 8(MAY), 172–184. <https://doi.org/10.4319/lom.2010.8.172>
- Takahashi, T., Sutherland, S. C., Wanninkhof, R., Sweeney, C., Feely, R. A., Chipman, D. W., et al. (2009). Climatological mean and decadal change in surface ocean pCO₂, and net sea-air CO₂ flux over the global oceans. *Deep-Sea Research Part II: Topical Studies in Oceanography*, 56(8–10), 554–577. <https://doi.org/10.1016/j.dsr2.2008.12.009>
- Williams, N. L., Juranek, L. W., Feely, R. A., Johnson, K. S., Sarmiento, J. L., Talley, L. D., et al. (2017). Calculating surface ocean pCO₂ from biogeochemical Argo floats equipped with pH: An uncertainty analysis. *Global Biogeochemical Cycles*, 31(3), 591–604. <https://doi.org/10.1002/2016GB005541>